ACS central science

Research Article

http://pubs.acs.org/journal/acscii

Carbon Nanotubes Produced from Ambient Carbon Dioxide for Environmentally Sustainable Lithium-Ion and Sodium-Ion Battery Anodes

Stuart Licht,*[,†] Anna Douglas,[‡] Jiawen Ren,[†] Rachel Carter,[‡] Matthew Lefler,[†] and Cary L. Pint*[,‡]

[†]Department of Chemistry, George Washington University, Washington, D.C. 20052, United States

[‡]Department of Mechanical Engineering, Interdisciplinary Materials Science Program, and Vanderbilt Institute of Nanoscale Science and Engineering, Vanderbilt University, Nashville, Tennessee 37235, United States

Supporting Information

ABSTRACT: The cost and practicality of greenhouse gas removal processes, which are critical for environmental sustainability, pivot on high-value secondary applications derived from carbon capture and conversion techniques. Using the solar thermal electrochemical process (STEP), ambient CO_2 captured in molten lithiated carbonates leads to the production of carbon nanofibers (CNFs) and carbon nanotubes (CNTs) at high yield through electrolysis using inexpensive steel electrodes. These low-cost CO_2-derived CNTs and CNFs are demonstrated as high performance energy storage materials in both lithium-ion and sodium-ion batteries. Owing to synthetic control of sp^3 content in the synthesized nanostructures, optimized storage capacities are measured over 370 mAh g^{-1} (lithium) and 130 mAh g^{-1} (sodium) with no capacity fade under durability tests up to 200 and 600 cycles, respectively. This work demonstrates that ambient CO_2, considered as an environmental pollutant, can be attributed economic value in grid-scale and portable energy storage systems with STEP scale-up practicality in the context of combined cycle natural gas electric power generation.

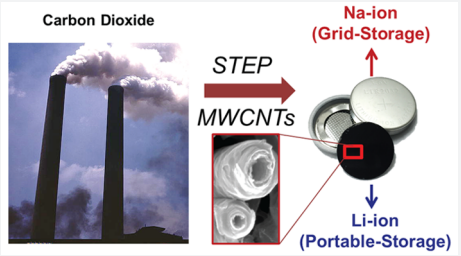

INTRODUCTION

A key challenge for atmospheric carbon capture and conversion technologies is the cost of operation or materials versus the perceived economic benefit to modern society. Issues such as stable carbon storage ultimately establish a cost and practicality bottleneck for many carbon capture processes.[1] Such issues can be resolved with the development of techniques that synergistically capture and convert atmospheric emissions into materials that can be developed into high-value products.[2] This produces a secondary market for greenhouse gas emissions and provides an economic value to pollutants that otherwise challenge the promise of long-term human sustainability on Earth.

In this manner, the elemental constituents of carbon dioxide, the most notable greenhouse gas, involve carbon and oxygen, which are foundational elemental building blocks for technological systems. Specifically, carbon-based materials are widely used in applications. One of the most notable applications of carbon is for anodes in lithium-ion (Li-ion) batteries, which are the principal rechargeable battery for electric vehicles (EVs) and consumer electronics.[3−5] Commercial Li-ion batteries most commonly rely on anodes produced with graphite that exhibit a theoretical Li-anode capacity of 1 Li: 6 C, or 372 mAh g^{-1},[5] and an observed capacity of 280−320 mAh g^{-1}.[6] Because of the greater Earth abundance of Na compared to Li (2.3% vs lithium's 0.0017% in the Earth's crust), recent efforts have also focused on carbon-based anodes for Na-ion battery systems.[7−9] A key challenge has been the low capacity of Na in crystalline carbons (32−35 mAh g^{-1}) which can be improved by introducing defects into the lattice or engineering the electrode−electrolyte interface to facilitate solvent-assisted intercalation.[10−12] Whereas other materials besides carbon can form low-potential compounds practical for Na-ion and Li-ion anodes, such as Si and Sn,[9,13] issues of rapid capacity fade, solid-electrolyte interphase vulnerability,[14] and existing commercial manufacturing infrastructure relevant to carbon-based anodes all present numerous technological challenges in transitioning battery systems away from carbon-based electrodes. Most recently, efforts to combine carbon-based Earth-abundant electrode materials, such as banana peels and peat moss, with sodium-ion batteries has been forward progress in this research area.[15,16]

In this report, we build upon the solar thermal electrochemical process (STEP),[17−21] which is designed to convert greenhouse gas carbon dioxide into a useful carbon commodity. This technique uses inexpensive electrode materials (galvanized steel cathode and a nickel anode) and molten carbonate electrolytes that are heated and powered using concentrated photovoltaic (CPV) cells that convert sunlight into electricity at 39% efficiency. STEP has been shown to function effectively with or without solar powered operation to electrolytically split water, carbon dioxide, or metal oxides,[22−24] produce STEP

Received: December 24, 2015
Published: March 2, 2016

DOI: 10.1021/acscentsci.5b00400
ACS Cent. Sci. 2016, 2, 162−168

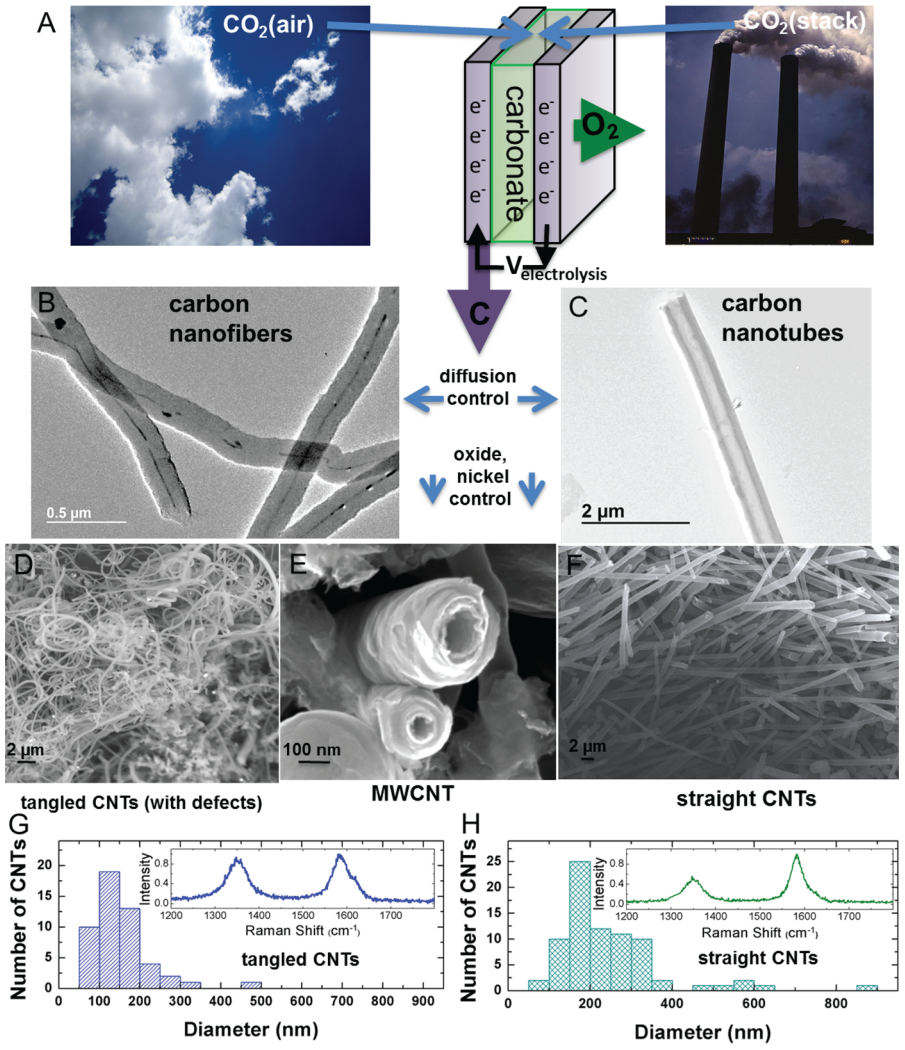

Figure 1. (A) Concept of high yield electrolytic synthesis of carbon nanostructures from dissolved air or smokestack concentrations of CO_2 in molten lithiated carbonates. During CO_2 electrolysis, transition metal deposition controls the nucleation and morphology of the carbon nanostructure. (B–C) SEM images depicting the different CNT products formed by controlled diffusion. SEM in (B) is from ^{13}C, and SEM in (C) is grown from natural abundance CO_2. (D–F) SEM images showing the different CNT morphologies formed based on either the addition of Li_2O (D - tangled, defective) or the absence of Li_2O (F - straight, less defective). (E) Edge-on high magnification view of STEP CNTs. (G, H) Diameter distribution of straight (G) and tangled (H) CNTs based on image analysis of SEM images, and Raman spectra of CNTs as used in this study and synthesized at 750 °C from natural abundance ^{12}C.

carbon,[18] produce STEP ammonia and STEP organic,[25−27] and produce STEP iron or cement.[28−30] Here we show that this process can be used as a sustainable synthetic pathway for defect-controlled CNT and CNF materials, which exhibit excellent performance in the context of lithium-ion and sodium-ion battery anode materials. This presents a sustainable route to convert carbon dioxide into materials relevant to both grid-scale and portable storage systems.

RESULTS AND DISCUSSION

The technique utilized to produce CNTs and CNFs from the STEP process is illustrated in Figure 1. In this study CNTs are grown by DC electrolysis from (natural isotope abundance) CO_2 dissolved in 750 °C molten Li_2CO_3 with, or without, added Li_2O. A 100 mL Ni crucible serves as both container and (O_2 generating) anode, and immersed 10 cm^2 galvanized steel as the cathode. The carbon product is characterized in the bottom of Figure 1. Following an initial low current (0.001 A for 0.5 h) step to grow Ni nucleation sites on the cathode, CNTs are grown on an immersed 10 cm^2 galvanized steel cathode at 1 A for 1 h. Two types of nanostructures are generated: straight CNTs that are grown in electrolyte without added Li_2O, and tangled CNTs that are grown when 4 m Li_2O has been added to the electrolyte.

The control of diffusion conditions during electrolytic splitting of CO_2 in molten lithium carbonate leads to either filled CNF or hollow CNT nanostructures, and control of oxide and transition metal concentration leads to tangled or straight fibers. This gives a level of control on the synthesized carbon nanostructures critical for battery applications. Specifically, the $^{13}CO_2$ and $Li_2{}^{13}CO_3$ CNF (Figure 1B) and 99% ^{12}C on the CNT (Figure 1C) illustrated are grown under similar conditions, but diffusion restraints of the heavier isotope allow more frequent Ni nucleation points, which can tend to fill the interior of the tube nanostructure. Similarly, both straight CNTs (Figure 1D) and tangled CNTs (Figure 1F) can be produced. The straight CNTs shown are grown without added oxide. Using this process, larger diameter CNTs can be

DOI: 10.1021/acscentsci.5b00400
ACS Cent. Sci. 2016, 2, 162−168

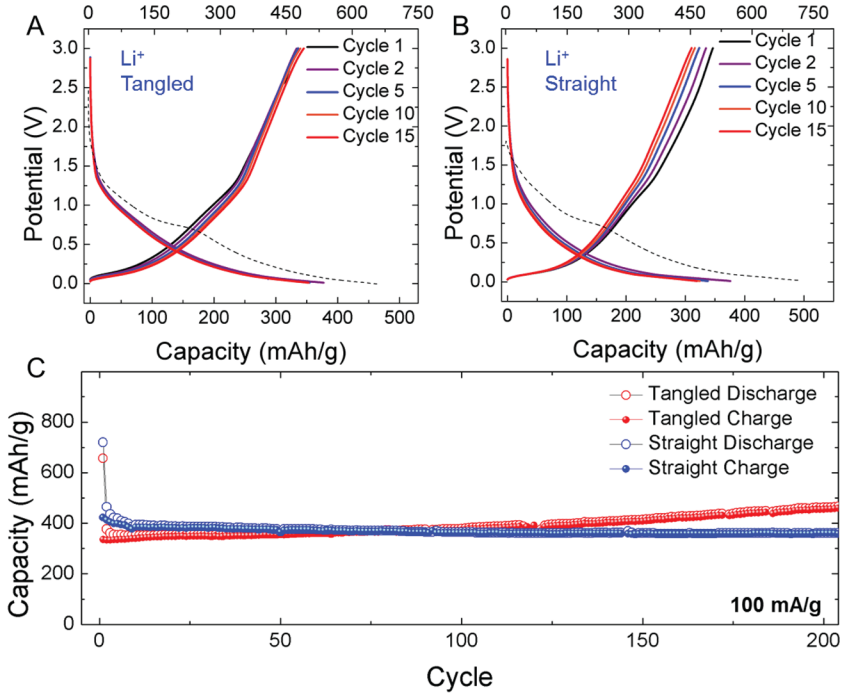

Figure 2. CO_2-derived Li-ion batteries. (A, B) First 15 galvanostatic charge−discharge profiles for CO_2-derived straight and tangled CNTs at a current density of 100 mA/g. The first discharge (dashed line) is longer than subsequent discharge cycles due to SEI formation and is referenced to the top axis in mAh/g. (C) Extended cycling performed at a current density of 100 mAh/g over 200 cycles for both straight and tangled CNTs.

obtained by pulsing the formation current for 9 min on (at 1 A) and 1 min off. The tangled CNTs shown are grown in high electrolytic oxide DC conditions.[18]

Raman spectroscopic analysis was carried out to study the degree of graphitization of the synthesized carbon nanostructures. In Figure 1, the Raman spectrum exhibits two sharp peaks observed at 1350 and 1580 cm^{-1}, which correspond to the disorder-induced mode (D band) and the high frequency E_{2g} first order mode (G band) that correspond generally to sp^3 and sp^2 hybridized carbon species, respectively. The intensity ratio between the D band and G band (I_D/I_G) is an important parameter to evaluate the graphitization and hence the total relative ratio of defective carbons in the material. As shown in Figure 1, the I_D/I_G ratio for tangled CNTs is significantly higher than straight CNTs—the latter of which is consistent with commercial hollow carbon nanofiber samples.[31] As we show in this study, synthetic control of the D:G ratio in a carbon material is useful to engineer the intercalation properties of carbon-based electrodes. Furthermore, based on a collection of SEM images of the as-grown tangled and straight CNTs, size distributions of the CNT materials were assigned based on ImageJ analysis software.[32] Size distributions indicate that the tangled CNTs exhibit a slightly overall smaller CNT diameter than the straight CNTs; however, all CNTs in this study are in a size range that is ideal for battery materials. The sizes of CNTs in this study (1) minimizes electrolyte consumption due to SEI formation in comparison to smaller nanostructured carbons and (2) enables full accessibility of the carbon material to alkali ion diffusion in thick, 3D electrode slurries.

To demonstrate the capability to transform CO_2 into a usable carbon material that can be assessed for energy storage applications, two types of CNTs, straight and tangled, were developed into electrodes, combined into half-cells along with electrolyte and a separator and pressed into coin cells for electrochemical testing. For Li-ion cells, CO_2-derived CNT electrodes were cast into a slurry with conductive carbon black and PVDF binder (3:1:1 ratio). This electrode was then combined with a separator, 1 M $LiPF_6$ in EC/DEC electrolyte, lithium metal foil, and pressed into a 2032 coin cell. Cyclic voltammetry tests (Supporting Information) and galvanostatic charge−discharge tests at rates of 100 mA/g elucidate the storage capability of both tangled (Figure 2A) and straight (Figure 2B) CO_2-derived CNTs. The first discharge, which is associated with solid electrolyte interphase (SEI) formation, is isolated from subsequent discharge cycles and plotted relative to the top axis in Figure 2A,B. For both the tangled and straight CNTs, subsequent cycling leads to high Coulombic efficiency (near 100%) and stable performance by the ∼15th cycle. In both cases, the reversible capacity on the second discharge is measured near 370 mAh g^{-1}, and this stabilizes near 350 mAh g^{-1} by the 15th cycle in both cases. To further assess the long-term performance of these materials, we carried out extended cycling tests at 100 mA/g (∼C/7.5) rates for 200 cycles, which extended for ∼2.5 months of continuous testing (Figure 2C). Here, a distinction between the storage behavior of straight (less defective) and tangled (higher defect content) CNTs emerges. Whereas the capacity of straight CNTs remains virtually unchanged over the cycling process, the storage capacity of the tangled CNTs is observed to steadily increase. After 200 cycles, the tangled CNT capacity is measured as ∼460 mAh g^{-1}, with the capacity of straight CNTs remaining invariant at ∼360 mAh g^{-1}. As such increased capacity above 372 mAh g^{-1},[33,34] and specifically during cycling,[35] has been reported in other studies on carbon nanostructured electrodes, our results imply this effect may be related to defect-induced modification to storage processes over the course of cycling. On the basis of the comparison of straight CNTs to tangled CNTs, the high defect content and torturous bends in the tangled CNTs likely could enable a transition from dilute staging of Li^+, which occurs during the formation of LiC_6,[36] to a combination

DOI: 10.1021/acscentsci.5b00400
ACS Cent. Sci. 2016, 2, 162−168

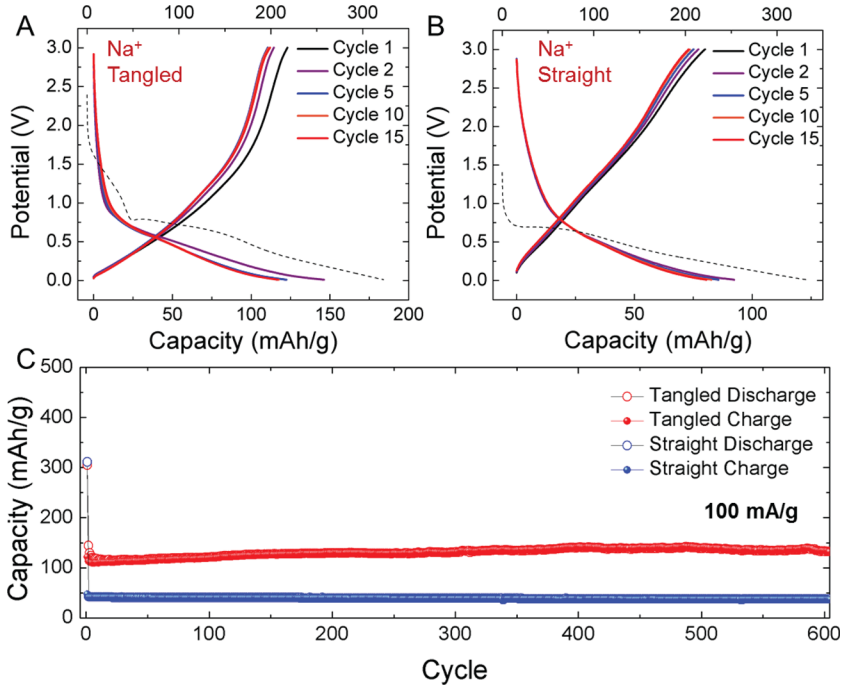

Figure 3. CO_2-derived Na-ion batteries. (A–B) First 15 galvanostatic charge–discharge profiles for CO_2-derived straight and tangled CNTs at current density of 100 mA/g. The first discharge (dashed line) is longer than subsequent discharge cycles due to SEI formation and is referenced to the top axis in mAh/g. (C) Extended cycling performed at current density of 100 mAh/g over 600 cycles for both straight and tangled CNTs.

of this and a mechanism analogous to pore-filling, which has been observed with other alkali-ion systems with very high defect-containing carbons.[11] The increased capacity over cycling emphasizes the continuous activation of this storage mode, which enables a capacity superior to the maximum alloying capacity of Li in LiC_6.

In addition to lithium-ion batteries, we also analyzed these materials as electrodes for Na^+ battery anodes. Recent efforts have been focused on Na^+ storage mechanisms into carbon materials,[11] and whereas some reports indicate intercalation,[15,16] often involving solvent cointercalation,[12] defect-containing carbon materials are known to achieve moderate Na^+ storage capacities based on a combined intercalation and pore-filling mechanism that only occurs with highly defective materials.[11] In this manner, the ability to modulate the defect density based on the STEP synthesis pathway enables a comparison that can elucidate this effect and highlights a synthetic trajectory toward high performance CO_2-derived sodium-ion battery electrodes for grid-scale applications. In this case, the batteries were prepared identically, except the electrolyte was based on 1 M $NaPF_6$ in diethylene glycol dimethyl ether (DGM), and the half-cells were cycled against Na foil counterelectrodes. Unlike the case of Li-ion cells, the Na-ion cells exhibit significantly different storage performance between the straight and tangled CNTs (Figure 3). In this case, galvanostatic charge–discharge data elucidates the straight CNTs to exhibit a reversible capacity that is only slightly higher than the maximum intercalation capacity of Na^+ in crystalline carbons. Whereas the I_D/I_G ratio is ~0.4, which implies a highly defective material relative to crystalline carbon, galvanostatic data indicate that this defect density is still too low to access a significant capacity of stored Na^+ in the context of pore-filling mechanism. However, the tangled CNTs, which exhibit a higher I_D/I_G ratio near 0.9, exhibit reversible capacities over 130 mAh g^{-1}, which is ~2× that of the straight CNTs. This implies defects in a CNT material are critical to activate the mechanism for Na^+ storage, and this is achieved in the tangled CNTs produced in the STEP process. To further assess the stability of this anode performance, both straight and tangled CNTs were cycled for 600 cycles at a similar rate of 100 mA/g. In parallel to Li-ion cells, this represents ~2.5 months of continuous cycling of the devices. Over the course of this cycling process, the devices show invariant performance with no observed capacity fade, which is improved compared to other defective carbon materials that exhibit storage via the pore-filling mechanism.[37] One possible explanation for this improved performance is a storage capacity that appears to originate mostly from the sloping part of the galvanostatic Na^+ insertion curve. Recent work by Bommier et al. has proposed that this sloping region is correlated with defect-activated sodium insertion in hard carbons.[11] This is distinguished from the flat, lower-voltage feature attributed primarily to plating of Na^+ on the interior of micropores in the anode. Our results are consistent with this picture since by increasing the defect density of the CNTs, the total capacity of the sloping region in the galvanostatic curves also similarly increases, but notably the flat signature at low voltages remains generally absent. Therefore, our results not only are in agreement with Bommier et al., but the invariant cycling performance observed over 600 cycles (~2.5 months) implies that defect-activated storage is highly reversible and not as prone to the capacity fade observed when sodium insertion occurs primarily through the plating mechanism. This implies that high capacity sodium-ion batteries with excellent cycling performance can be rationally designed by controlling structural and defect properties of the carbons. Results from cyclic voltammetry scans and rate capability tests of these materials are available in the Supporting Information.

Overall, electrochemical tests give promise to the function of CO_2-derived CNTs as practical anode materials for batteries. This establishes the principle that energy input can transform

DOI: 10.1021/acscentsci.5b00400
ACS Cent. Sci. 2016, 2, 162–168

CO_2, which is a global pollutant with adverse environmental impact, into a secondary product that now is associated with an economic value in a thriving technological area. In order to illustrate this point, simple calculations were performed based on available data in the literature to correlate the average value of CO_2 in batteries based upon the total cost per kWh of the battery cell (Figure 4). Unlike routes to transform CO_2 into fuels such as methanol, which targets a low-value hydrocarbon commodity, the transformation of CO_2 into active battery materials provides a valuation of the CO_2 that is associated with the total cost of the battery technology. The U.S. Department of Energy Vehicle Technology Office (FY 2015 Budget Outlook[38]) has set a target of $125 per kWh by year 2022, with an average battery cost of ~$325 per kWh in 2013. These calculations, which are very generalized and can widely vary based on battery manufacturing techniques, battery size, and packaging processes, build upon the assumptions that (1) ~8% of the total battery cost is associated with the anode,[39] (2) the total mass of anodic carbon in a 1 kWh module is <10% of the total weight of the battery, (3) the mass extrapolated for a 1 kWh module is ~5.3 kg (e.g., Panasonic 18650 type 1.5 kWh modules), and (4) processes to convert CO_2 to functional carbon materials transform all carbon into usable material. This explicitly demonstrates an operation window for large-scale processes capable of converting CO_2 into carbon-based battery anodes and explicitly demonstrates the principle that CO_2 can be associated with economic value in a growing technological sector.

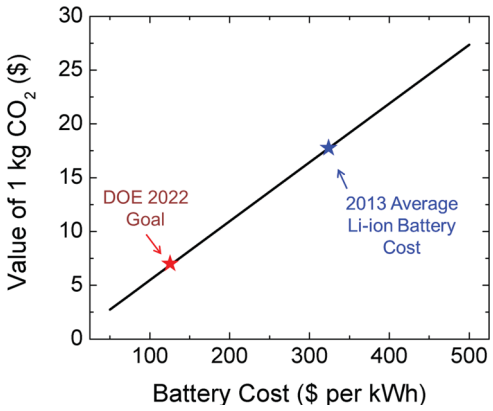

Figure 4. Generalized value of 1 kg CO_2 converted into CNT materials for batteries based on the total cost per kWh for the battery. The DOE target of $125/kWh for 2022 and the 2013 average Li-ion battery cost provide a window ranging from ~$5 to $18 of secondary value per kg of CO_2. Anode cost relative to the full cell is extrapolated from data in ref 39, and weight per kWh is extrapolated from a Panasonic 1.5 kWh (52 Ah) module.

In this spirit, two possibilities emerge to produce materials derived from CO_2 that can have economic value in battery systems: ambient atmospheric capture of CO_2 or the extraction of CO_2 from industrial smokestacks, such as from conventional fossil fuel power plants. The energy costs of the latter based on combined cycle (CC) natural gas plants are discussed in brief. Rather than processing large volumes to transform CO_2 from air, the CO_2 is available at higher concentration, and not only provides the hot CO_2 for dissolution in the electrolysis, but also removes CO_2 from the plant emission. Additionally, the electrolysis provides a pure oxygen product for improved power plant combustion efficiency. Figure 5A illustrates action of a conventional CC electrical power plant which emits a flue gas that contains ~9% CO_2. The conventional CC plant increases the fuel to electricity efficiency compared to single cycle electrical power plants by directing the exhaust heat emissions from a gas (Brayton cycle) electrical turbine to boil water to power a steam (Rankine cycle) electrical turbine.

As shown in Figure 5B, an alternative CNT CC plant product provides a platform for the simplified CNT cost analysis, and in addition to electricity, simultaneously produces

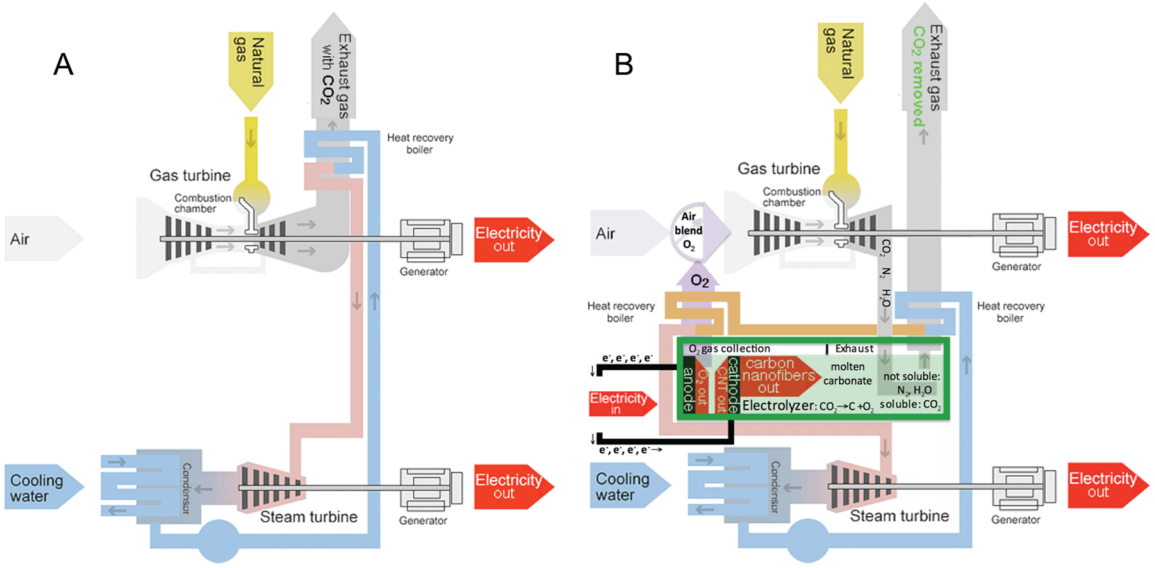

Figure 5. Action of a conventional CC power plant which has an exhaust with CO_2 (A) compared to the introduced CNF CC power plant with the carbon dioxide removed from the exhaust gas (B).[40] Left (A) The conventional gas/steam combined cycle CC power plant is illustrated as modified from ref 41. Right (B) The CC CNF power plant described in this study, illustrating the CNF (including carbon nanofibers or carbon nanotube) product, the electrolysis pure oxygen cycled back into the gas combustion, recovered heat to the steam turbine and carbon dioxide removed from the exhaust gas.

DOI: 10.1021/acscentsci.5b00400
ACS Cent. Sci. 2016, 2, 162−168

a valuable carbon nanofiber product. Unlike the conventional CC (Figure 5A), CO_2 is removed from the exhaust of the CNT CC power plant on the right. As shown, the hot CO_2, N_2, and H_2O CC emission is instead bubbled into molten carbonate where only the CO_2 dissolves. The remaining gases (with the CO_2 removed) become the exhaust gas (after heat recovery). The dissolved CO_2 is split by electrolysis into oxygen gas at the anode, which is fed (after heat recovery) back into the gas turbine and carbon (CNT) at the cathode. The CNT product can hence be tuned for strength, diameter, length, defect-content, geometry, and electrical or thermal conductivity by the specific molten salt electrochemistry employed. The CNT product may be removed periodically or as a constant throughput). The recovered heat boils water to power a steam turbine to also generate electricity. Heat is returned to the steam generator chamber using (i) heat recovered from the electrolysis (pure oxygen and carbon nanofiber) products, and (ii) from the carbon dioxide removed electrolysis exhaust.

The CNT CC natural gas to electricity plant efficiency is increased by the "free" pure oxygen generated during the CNT production by electrolysis by increasing the natural gas combustion temperature compared to the more dilute oxygen in air and contributes to an offset of the energy required to drive the electrolysis. The heated CO_2 reactant is provided by the plant, and the electrical energy required to drive the electrolysis of CO_2 is recovered many fold by the increased value of the CNT product (e.g., Figure 5) compared to the cost of the natural gas consumed. Electrolysis costs to produce CNTs will be similar to infrastructure costs associated with the chlor-alkali and aluminum industries. The electrical energy costs to prepare the CNFs are low, requiring 0.9 to 1.4 V.[21] CNFs are consistently prepared here at 80 to 100% Coulombic efficiency of the four electrons required to reduce CO_2, which at $0.10 per kWh is equivalent to $800 to $1,600 per metric tonne of CNT—leading to high revenue windows for battery applications. Lithium carbonate is not consumed during the CO_2 electrolysis and at today's cost of $6,000 per ton, as amortized over 10 year's usage, cost an additional $140 per metric tonne CNT. These costs compare to today's cost of $200,000 to 400,000 per metric tonne of industrial grade (90% purity) CNTs. The production of CNTs by electrolysis provides a low-cost pathway for CNTs and hence gives an economically practical trajectory toward the conversion of CO_2 into battery materials.

CONCLUSIONS

Here we report the transformation of CO_2 into low-defect (straight) and higher defect (tangled) CNT materials for use in both lithium-ion and sodium-ion batteries using the STEP process. These battery materials show excellent performance and durability, with no capacity fade measured in over 2.5 months of continuous cycling, corresponding to over 200 cycles and 600 cycles for lithium-ion and sodium-ion devices, respectively. Control on the defect density was observed to be critical to enable capacities that surpass LiC_6 in Li-ion cells and overcome the bottleneck of 30−40 mAh/g capacity in sodium-ion cells that is associated with carbon materials. This provides a bridge toward associating economic value to CO_2, with a revenue window controlled by the cost of conventional battery technology per kWh. Processes to scale this STEP technique to levels of industrial CO_2-containing smokestacks give promise for high energy efficiency CNT production through the STEP process with a STEP byproduct of O_2 that can aid combustion.

ASSOCIATED CONTENT

Supporting Information

The Supporting Information is available free of charge on the ACS Publications website at DOI: 10.1021/acscentsci.5b00400.

(i) Additional experimental details, and (ii) cyclic voltammetry and rate capability data for CO_2-derived battery electrodes (PDF)

AUTHOR INFORMATION

Corresponding Authors

*(S.L.) E-mail: slicht@gwu.edu.

*(C.L.P.) E-mail: cary.l.pint@vanderbilt.edu.

Notes

The authors declare no competing financial interest.

ACKNOWLEDGMENTS

We thank Rizia Bardhan for use of the Raman microscope critical for this work. S.L. is grateful for partial support of this research by NSF Grants Nos. 1230732 and 1505830. A.D. is supported by the National Science Foundation Graduate Research Fellowship under Grant No. 1445197.

REFERENCES

(1) Leung, D. Y. C.; Caramanna, G.; Maroto-Valer, M. M. An Overview of Current Status of Carbon Dioxide Capture and Storage Technologies. *Renewable Sustainable Energy Rev.* **2014**, *39*, 426−443.

(2) Lim, X. Z. How to Make the Most of Carbon Dioxode. *Nature* **2015**, *526*, 628−630.

(3) Dunn, B.; Kamath, H.; Tarascon, J. M. Electrical Energy Storage for the Grid: A Battery of Choices. *Science* **2011**, *334*, 928−935.

(4) Tarascon, J. M. Is lithium the new gold? *Nat. Chem.* **2010**, *2*, 510−510.

(5) Nitta, N.; Wu, F. X.; Lee, J. T.; Yushin, G. Li-ion battery materials: present and future. *Mater. Today* **2015**, *18*, 252−264.

(6) Xiong, Z.; Yun, Y. S.; Jin, H. J. Applications of Carbon Nanotubes for Lithium Ion Battery Anodes. *Materials* **2013**, *6*, 1138−1158.

(7) Kundu, D.; Talaie, E.; Duffort, V.; Nazar, L. F. The Emerging Chemistry of Sodium Ion Batteries for Electrochemical Energy Storage. *Angew. Chem., Int. Ed.* **2015**, *54*, 3431−3448.

(8) Palomares, V.; Casas-Cabanas, M.; Castillo-Martinez, E.; Han, M. H.; Rojo, T. Update on Na-based battery materials. A growing research path. *Energy Environ. Sci.* **2013**, *6*, 2312−2337.

(9) Yabuuchi, N.; Kubota, K.; Dahbi, M.; Komaba, S. Research development on sodium-ion batteries. *Chem. Rev.* **2014**, *114*, 11636−11682.

(10) Zhu, Z.; Cheng, F.; Hu, Z.; Niu, Z.; Chen, J. Highly stable and ultrafast electrode reaction of graphite for sodium ion batteries. *J. Power Sources* **2015**, *293*, 626−634.

(11) Bommier, C.; Surta, T. W.; Dolgos, M.; Ji, X. New Mechanistic Insights on Na-Ion Storage in Nongraphitizable Carbon. *Nano Lett.* **2015**, *15*, 5888−5892.

(12) Cohn, A. P.; Share, K.; Carter, R.; Oakes, L.; Pint, C. L. Ultrafast Solvent-Assisted Sodium Ion Intercalation into Highly Crystalline Few-Layered Graphene. *Nano Lett.* **2016**, *16*, 543−548.

(13) Su, X.; Wu, Q. L.; Li, J. C.; Xiao, X. C.; Lott, A.; Lu, W. Q.; Sheldon, B. W.; Wu, J. Silicon-Based Nanomaterials for Lithium-Ion Batteries: A Review. *Adv. Energy Mater.* **2014**, *4*, 1300882.

(14) Menkin, S.; Golodnitsky, D.; Peled, E. Artificial solid-electrolyte interphase (SEI) for improved cycleability and safety of lithium-ion cells for EV applications. *Electrochem. Commun.* **2009**, *11*, 1789−1791.

(15) Ding, J.; Wang, H. L.; Li, Z.; Kohandehghan, A.; Cui, K.; Xu, Z. W.; Zahiri, B.; Tan, X. H.; Lotfabad, E. M.; Olsen, B. C.; et al. Carbon

DOI: 10.1021/acscentsci.5b00400
ACS Cent. Sci. 2016, 2, 162−168

Nanosheet Frameworks Derived from Peat Moss as High Performance Sodium Ion Battery Anodes. *ACS Nano* **2013**, *7*, 11004−11015.
(16) Lotfabad, E. M.; Ding, J.; Cui, K.; Kohandehghan, A.; Kalisvaart, W. P.; Hazelton, M.; Mitlin, D. High-Density Sodium and Lithium Ion Battery Anodes from Banana Peels. *ACS Nano* **2014**, *8*, 7115−7129.
(17) Licht, S. STEP (Solar Thermal Electrochemical Photo) Generation of Energetic Molecules: A Solar Chemical Process to End Anthropogenic Global Warming. *J. Phys. Chem. C* **2009**, *113*, 16283−16292.
(18) Ren, J. W.; Li, F. F.; Lau, J.; Gonzalez-Urbina, L.; Licht, S. One-Pot Synthesis of Carbon Nanofibers from CO2. *Nano Lett.* **2015**, *15*, 6142−6148.
(19) Licht, S.; Wang, B. H.; Wu, H. J. STEP-A Solar Chemical Process to End Anthropogenic Global Warming. II: Experimental Results. *J. Phys. Chem. C* **2011**, *115*, 11803−11821.
(20) Licht, S.; Wang, B. H.; Ghosh, S.; Ayub, H.; Jiang, D. L.; Ganley, J. A New Solar Carbon Capture Process: Solar Thermal Electrochemical Photo (STEP) Carbon Capture. *J. Phys. Chem. Lett.* **2010**, *1*, 2363−2368.
(21) Ren, J. W.; Lau, J.; Lefler, M.; Licht, S. The Minimum Electrolytic Energy Needed To Convert Carbon Dioxide to Carbon by Electrolysis in Carbonate Melts. *J. Phys. Chem. C* **2015**, *119*, 23342−23349.
(22) Licht, S. Efficient Solar-Driven Synthesis, Carbon Capture, and Desalinization, STEP: Solar Thermal Electrochemical Production of Fuels, Metals, Bleach. *Adv. Mater.* **2011**, *23*, 5592−5612.
(23) Li, F. F.; Liu, S. Z.; Cui, B. C.; Lau, J.; Stuart, J.; Wang, B. H.; Licht, S. Solar Fuels: A One-Pot Synthesis of Hydrogen and Carbon Fuels from Water and Carbon Dioxide. *Adv. Energy Mater.* **2015**, *5*, 1401791.
(24) Licht, S.; Halperin, L.; Kalina, M.; Zidman, M.; Halperin, N. Electrochemical potential tuned solar water splitting. *Chem. Commun.* **2003**, 3006−3007.
(25) Licht, S.; Cui, B. C.; Wang, B. H.; Li, F. F.; Lau, J.; Liu, S. Z. Ammonia synthesis by N-2 and steam electrolysis in molten hydroxide suspensions of nanoscale Fe2O3. *Science* **2014**, *345*, 637−640.
(26) Li, F. F.; Licht, S. Advances in Understanding the Mechanism and Improved Stability of the Synthesis of Ammonia from Air and Water in Hydroxide Suspensions of Nanoscale Fe2O3. *Inorg. Chem.* **2014**, *53*, 10042−10044.
(27) Zhu, Y. J.; Wang, B. H.; Liu, X. L.; Wang, H. Y.; Wu, H. J.; Licht, S. STEP organic synthesis: an efficient solar, electrochemical process for the synthesis of benzoic acid. *Green Chem.* **2014**, *16*, 4758−4766.
(28) Cui, B. C.; Licht, S. Critical STEP advances for sustainable iron production. *Green Chem.* **2013**, *15*, 881−884.
(29) Licht, S.; Wu, H. J. STEP Iron, a Chemistry of Iron Formation without CO_2 Emission: Molten Carbonate Solubility and Electrochemistry of Iron Ore Impurities. *J. Phys. Chem. C* **2011**, *115*, 25138−25147.
(30) Licht, S.; Wu, H. J.; Hettige, C.; Wang, B. H.; Asercion, J.; Lau, J.; Stuart, J. STEP cement: Solar Thermal Electrochemical Production of CaO without CO_2 emission. *Chem. Commun.* **2012**, *48*, 6019−6021.
(31) Saravanan, M.; Sennu, P.; Ganesan, M.; Ambalavanan, S. Multi-Walled Carbon Nanotubes Percolation Network Enhanced the Performance of Negative Electrode for Lead-Acid Battery. *J. Electrochem. Soc.* **2013**, *160*, A70−A76.
(32) Schneider, C. A.; Rasband, W. S.; Eliceiri, K. W. NIH Image to ImageJ: 25 years of image analysis. *Nat. Methods* **2012**, *9*, 671−675.
(33) Lahiri, I.; Oh, S. W.; Hwang, J. Y.; Cho, S.; Sun, Y. K.; Banerjee, R.; Choi, W. High Capacity and Excellent Stability of Lithium Ion Battery Anode Using Interface-Controlled Binder-Free Multiwall Carbon Nanotubes Grown on Copper. *ACS Nano* **2010**, *4*, 3440−3446.
(34) Carter, R.; Oakes, L.; Cohn, A. P.; Holzgrafe, J.; Zarick, H. F.; Chatterjee, S.; Bardhan, R.; Pint, C. L. Solution Assembled Single-Walled Carbon Nanotube Foams: Superior Performance in Supercapacitors, Lithium-Ion, and Lithium-Air Batteries. *J. Phys. Chem. C* **2014**, *118*, 20137−20151.
(35) Fan, Z. J.; Yan, J.; Ning, G. Q.; Wei, T.; Zhi, L. J.; Wei, F. Porous graphene networks as high performance anode materials for lithium ion batteries. *Carbon* **2013**, *60*, 558−561.
(36) Inaba, M.; Yoshida, H.; Ogumi, Z.; Abe, T.; Mizutani, Y.; Asano, M. In situ Raman study on electrochemical Li intercalation into graphite. *J. Electrochem. Soc.* **1995**, *142*, 20−26.
(37) Cao, Y.; Xiao, L.; Sushko, M. L.; Wang, W.; Schwenzer, B.; Xiao, J.; Nie, Z.; Saraf, L. V.; Yang, Z.; Liu, J. Sodium ion insertion in hollow carbon nanowires for battery applications. *Nano Lett.* **2012**, *12*, 3783−3787.
(38) Vehicle Technologies Office FY 2015 Budget at-a-Glance; U.S. Department of Energy: Washington, D.C., 2014; http://energy.gov/sites/prod/files/2014/03/f9/fy15_at-a-glance_vto.pdf.
(39) Wood, D. L.; Li, J. L.; Daniel, C. Prospects for reducing the processing cost of lithium ion batteries. *J. Power Sources* **2015**, *275*, 234−242.
(40) Licht, S.Carbon Nanofiber Electric and Heat Power Plants, U.S. Provisional Patent 62/240,805, October 13, 2015.
(41) eon.co, accessed November 9, 2015 at http://www.eon.com/en/business-areas/power-generation/natural-gas-and-oil/combined-cycle-gas-turbine-how-it-works.html.

DOI: 10.1021/acscentsci.5b00400
ACS Cent. Sci. 2016, 2, 162−168